On the fundamental resonant mode of inhomogeneous soil deposits

Joaquin Garcia-Suarez[1]

Graduate Aerospace Laboratories, Caltech, Pasadena, CA, 91125

Domniki Asimaki

Mechanical and Civil Engineering, Caltech, Pasadena, CA, 91125

Abstract

The problem of estimating seismic ground deformation bears paramount importance to engineers designing and maintaining infrastructure in earthquake-prone areas. Notwithstanding its vital importance, the quantification of this deformation is still an open research area that concerns from engineers to seismologists and geophysicist. Particularly, the problem of finding the displacement field in a soft shallow layer overlying rigid bedrock induced by simple SH wave excitation has been favored by engineers due to its simplicity combined with inherent relevance for practical scenarios. This document furnishes accurate estimates for both the fundamental frequency and the amplitude of the first resonant mode which does not require considering a continuous inhomogeneity distribution. These are attained through application of a new physical argument based on resonance of single-degree-of-freedom systems.

Keywords: Site Response Analysis, Resonance, Soil Deposit

---

1. Introduction

Benuska [1] established that site conditions and soil layering have meaningful effects over ground motions during seismic events. The evolution of mechanical

Email addresses: ajgarcia@caltech.edu (Joaquin Garcia-Suarez), domniki@caltech.edu (Domniki Asimaki)

[1]Corresponding author.

properties in the soil can induce a concentration of seismic energy in the softer layers [2], which usually are those closer to the surface, and in turn translates into higher risk for man-made above-ground and underground structures.

Consequently, a number of researchers have been occupied with studying the modification of ground seismic response due to the presence of inhomogeneous stratification in the soil by means of simplified one dimensional (1D) wave propagation models under the assumption of linear-elastic medium [3, 4, 5, 6, 7, 8, 9, 10], which happens to be appropriate when

1) small strains in the soil ergo the material response remains linear-elastic (absence non-linear material phenomena),
2) the soil is layered vertically (thus the problem reduces to one-dimensional, vertical, wave propagation),
3) vertically-ascending SH waves conform the excitation,
4) material internal damping is frequency-independent.

The customary approach focuses on finding steady-state solution in frequency domain, which happens to be the dominant component of the response, except under some specific circumstances (low-frequency fundamental mode, high-frequency excitation [11]).

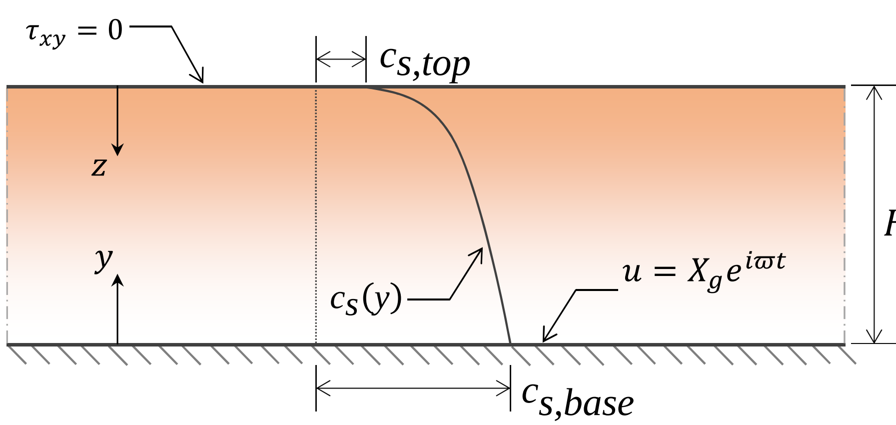

Figure 1: Scheme of the system considered in this study.

1.1. The governing equations

The harmonic wave-propagation problem to be considered, in terms of the total displacement amplitude $\hat{u}_t$, is [12]

$$\frac{d}{dz}\left[\mu(z)\frac{d\hat{u}_t}{dz}\right] + \rho\varpi^2\hat{u}_t = 0 \qquad \text{s.t.} \qquad \hat{u}_t(z = H) = X_g \quad , \quad \left.\frac{d\hat{u}_t}{dz}\right|_{z=0} = 0\,, \tag{1}$$

where z is the coordinate stretching from the free surface to the rigid base, ρ represents the density of the soil (which is assumed to remain constant), the seismic S-wave excitation is modeled as a uniform displacement at the soil base $X_g e^{i\varpi t}$, and $\mu(z)$ represents the variation of shear modulus with depth. Damping is not shown explicitly in eq. (1) as it is not of the viscous type but hysteretic, hence the shear modulus is interpreted as an storage modulus (real number) plus a loss modulus (imaginary number) as $\mu(z) \to \mu(z)(1 + \mathrm{i}\delta_d)$, where δ_d is referred as coefficient of material damping.

For the sake of clarity, let us restate that the time variation is taken as given by $e^{i\varpi t}$, hence both X_g and $\hat{u}_t$ are the *amplitudes* that accompany the phase: X_g is a positive real number, whereas $\hat{u}_t$ represents a complex number whose modulus is the total displacement magnitude and whose argument represents the time shift between load (input) and displacement (response, output).

The prior equation is classified as an homogeneous ODE of the Helmhotz-type with inhomogeneous boundary conditions. By introducing $\hat{u} = \hat{u}_t - X_g$, the *relative-to-base* horizontal displacement amplitude, and $y = H - z$, the complementary coordinate to z, the problem (1) becomes

$$\frac{d}{dy}\left[\mu(y)\frac{d\hat{u}}{dy}\right] + \rho\varpi^2\hat{u} = \rho\ddot{X}_g \qquad \text{s.t.} \qquad \hat{u}(y = 0) = 0 \quad , \quad \left.\frac{d\hat{u}}{dy}\right|_{y=H} = 0\,, \tag{2}$$

which represents the same phenomenon, although in a subtly, yet consequential, different way: instead of a homogeneous equation, now a *forced* Helmhotz equation with homogeneous boundary conditions is obtained. This fact will come in handy later.

1.2. Modeling the distribution of mechanical properties across depth

The main difficulty when it comes to obtaining and understanding the solution of either prior equations is the complex shape of the evolution of mechanical properties along the stratum in realistic scenarios, that is $\mu(y) = \rho c_s(y)^2 = \rho c_{s,base} f(\eta)$, $c_s(y)$ being a function that supplies the value of the S-wave velocity at any point in the stratum ($c_{s,base}$ corresponds to the value at the base, right before the bedrock), η the dimensionless vertical coordinate and $f(\eta)$ the function that describes the evolution along the deposit (see that $f(0) = 1$ and $f(1) = \beta = c_{s,top}/c_{s,base}$). This difficulty hinders the procurement of simple closed-form solutions for the natural frequencies and the displacement field in the stratum.

A widely-used expression for this evolution, since it lends itself to analytical treatment, is the so-called "generalized-parabola evolution", given by

$$\frac{c_s(z)}{c_{s,base}} = \sqrt{\frac{\mu(y)}{\mu_{base}}} = \left(b + (1-b)\,\frac{z}{H}\right)^n = \left(1 + \left(\beta^{1/n} - 1\right)\frac{y}{H}\right)^n , \tag{3}$$

where $b = \beta^{1/n} = (c_{s,top}/c_{s,base})^{1/n}$ and n is dubbed "inhomogeneity factor" (also referred to as "inhomogeneity parameter" [13]). The parameter b controls the maximum variation of c_s, which in this case always corresponds to top-to-bottom or vice versa, since the function only allows for monotonic evolution across the layer.

1.3. Previous results by Mylonakis, Rovithis and Parashakis

Mylonakis and collaborators [14] proposed applying the Rayleigh quotient of the governing ODE eq. (1), to estimate the natural frequencies:

$$\mathcal{R}^2 = \frac{\int_0^1 f^2(\eta)\left(\frac{d\psi_1(\eta)}{d\eta}\right)^2 d\eta}{\int_0^1 \psi_1^2(\eta) d\eta} \approx \left(\frac{\omega_s}{c_{s,base}/H}\right)^2 , \tag{4}$$

where ω_s represents the fundamental frequency of the system, $\eta = y/H$ is a dimensionless vertical displacement, ψ_1 is a shape function that must be pointwise-similar to the fundamental shape in order for the estimation to work, and $f(\eta) = c_s(y)/c_{s,base}$ is a dimensionless S-wave velocity evolution along the layer. The method relies on "guessing" a good approximation of the first mode shape, but it appears that using simple profiles, as parabolic or sinusoidal, fulfils to obtain good results, at least in those models conforming to the eq. (3) (check Figure 5 in order to gauge these assertions).

The same authors also provided an exact solution of eq. (2) when $f(\eta)$ is given by eq. (3) [12]. They found that the total displacement evolution was given by

$$\frac{\hat{u}_t}{X_g} = (b+q(1-\eta))^{\psi}\left[\frac{J_{\nu+1}(\lambda b^{\ell/2})Y_{\nu}\left(\lambda(b+q(1-\eta))^{\ell/2}\right)}{J_{\nu+1}(\lambda b^{\ell/2})Y_{\nu}(\lambda)-J_{\nu}(\lambda)Y_{\nu+1}(\lambda b^{\ell/2})}\right. \\ \left. -\frac{J_{\nu}\left(\lambda(b+q(1-\eta))^{\ell/2}\right)Y_{\nu+1}(\lambda b^{\ell/2})}{J_{\nu+1}(\lambda b^{\ell/2})Y_{\nu}(\lambda)-J_{\nu}(\lambda)Y_{\nu+1}(\lambda b^{\ell/2})}\right], \tag{5}$$

where J_i and Y_i are the Bessel functions of i-th kind, $\ell = 2(1-n)$, $\psi = (1-2n)/2$, $\nu = (2n-1)/2(1-n)$, $\lambda = 2r/\ell(1-b)$, $q = 1-b$, and $r = \varpi H/c_{s,base}$. See that the frequency dependence occurs by means of the function $\lambda = \lambda(r) = \lambda(\varpi)$, which should not be mistaken by either the Lamé constant or a wavelength. In order to stress the significant complexity of eq. (5), and also for a discussion to be tackled later in this text, let us also show the displacement field corresponding to a homogeneous layer [15]:

$$\frac{\hat{u}_t(\eta)}{X_g} = \frac{\cos\left(\frac{\varpi H}{c_s}(1-\eta)\right)}{\cos\left(\frac{\varpi H}{c_s}\right)} \rightarrow \tag{6a}$$

$$\frac{|\hat{u}(\eta)|}{X_g} = \left|\frac{\hat{u}_t(\eta)}{X_g} - 1\right| = \left|\frac{\cos\left(\frac{\varpi H}{c_s}(1-\eta)\right)}{\cos\left(\frac{\varpi H}{c_s}\right)} - 1\right|. \tag{6b}$$

Still focusing specifically on profiles given by eq. (3), the exact amplitude of the base-to-top transfer function was also provided by simply particularizing the eq. (5) at $\eta = 1$:

$$A_{exact}(b,n,r) = \frac{u_t(z=0)}{X_g} = \\ = \frac{2}{\pi}\frac{b^{\psi-\ell/2}}{\lambda}\left[J_{\nu+1}(\lambda b^{\ell/2})Y_{\nu}(\lambda) - J_{\nu}(\lambda)Y_{\nu+1}(\lambda b^{\ell/2})\right]^{-1}, \tag{7}$$

where the parameters this function depends where introduced with eq. (5). Therefore, the exact natural frequencies of the inhomogeneous system with $f(\eta)$ abiding by eq. (3) are found are the roots of the denominator of eq. (7) (the bracketed factor).

1.4. Previous results by Garcia-Suarez, Esmaeilzadeh and Asimaki

Likewise, estimate particularly well-suited for the high-frequency regime has been furnished previously by the authors [16]. Reagarding the base-to-top amplification, it was found

$$A_{asy}(\beta, n, r) = \frac{\sqrt{c_{s,base}/c_{s,top}}}{\cos\left(\frac{\varpi}{c_{s,eq}/H}\right)} , \tag{8}$$

where $c_{s,eq}$ represents the harmonic mean of the distribution $c_s(z)$:

$$c_{s,eq} = \left(\int_0^H \frac{d(z/H)}{c_s(z)}\right)^{-1} . \tag{9}$$

These results were derived through analysis of the exact solution eq. (7). The relation between the high-frequency limit of the exact solution and the so-called *nominal frequency of the site* [7] (the fundamental frequency of the homogeneous system having constant wave velocity given as eq. (9)) was established mathematically, what allowed to specify the validity conditions for the approximation to hold. The natural frequencies of the site (particularly the higher modes) can be approximated as

$$\omega_k = (2k-1)\frac{\pi}{2}\frac{c_{s,eq}}{H} , \tag{10}$$

for $k = 1, 2, 3, \ldots$

2. Derivation of estimates for the fundamental mode response

Given the system depicted in Section 1, governed by eq. (1), we would like to find estimates for the displacement field and the natural frequency concerning not the whole range of possible dynamic behavior but only the fundamental (viz. the first) resonant mode. To fulfil this endeavor, the following approach is proposed.

2.1. An "easing" argument based on single-degree-of-freedom resonance

See that eq. (2) represents but a classic equation of a one-degree-of-freedom system, wherein elastic, damping, and inertial forces team up to balance an external load [17].

It may not be so easy to appraise this as the damping is not of viscous type but hysteretic, so let us show it clearly by explicitly substituting $\mu(y)$ by $\mu(y)(1 + \mathrm{i}\delta_d)$ in eq. (2) (at this point let us also allow for evolving density, $\rho = \rho(y)$, too):

$$\frac{d}{dy}\left(\mu(y)\frac{d\hat{u}}{dy}\right) + \mathrm{i}\delta_d \frac{d}{dy}\left(\mu(y)\frac{d\hat{u}}{dy}\right) + \rho(y)\varpi^2\hat{u} = \rho(y)\ddot{X}_g\,. \tag{11}$$

Now it is easy to recognize each term in the left-hand side: from left to right, the first addend corresponds to elastic forces, the second one to hysteretic damping forces and the third to inertial forces, while the right-hand side is the "external body force". The diagrams in Figure 2 represents two possible admissible configurations in eq. (11):

- To the left, a configuration wherein elastic forces are dominant and hence, for the most part, these take care of balancing the external load (*low-frequency regime*). See that elastic force magnitude rely on straining (gradient of displacements), and thus large displacements are not necessarily required to balance the excitation, only enough *change* from point to point. Damping and inertial forces remain relatively small. See also that the phase difference between inertial and elastic forces is π rad, that is, half a period.

- To the right, a configuration we may refer as *resonance*: the elastic forces and the inertial forces reach equal magnitude, and, since they are out of phase, cancel each other, leaving the damping force solely in charge of compensating the external load. Given that δ_d tends to be small ($\delta_d \ll 1$ usually), it follows that the gradient magnitude must surge to compensate the detrimental influence of δ_d, but in this situation the magnitudes of both displacement and displacement gradient are directly linked through the condition of inertia balancing elastic forces, and thus the displacement amplitude surges as well.

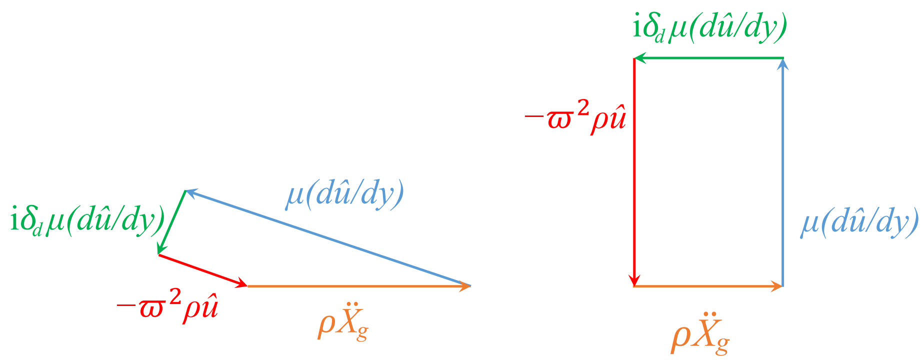

Figure 2: Schematic representation of two possible equilibria (red = inertial forces, green = damping forces, blue = elastic forces , orange = external load).

In conclusion, let us, from this point onward, consider resonance as the dynamic setting wherein elastic and inertial forces cancel each other (as they attain the same magnitude but their phases are shifted π radians), thus leaving the damping forces on their own to balance the "external" loading. In such a scenario we may particularize eq. (11) as

$$\mathrm{i}\delta_d \frac{d}{dy}\left(\mu(y)\frac{d\hat{u}}{dy}\right) = \rho(y)\ddot{X}_g \,. \tag{12}$$

This equation can be integrated right away to yield the horizontal displacement field along the layer when $\varpi = \omega_s$. Note how in these developments we have not required of continuity or smoothness conditions to be laid over the distribution mechanical properties), it is only requested that the function is positive (so it can be inverted) and that its inverse is such as to allow the subsequent integration. Proceeding with the integration and imposing the boundary conditions in (2) one attains the displacement at resonance

$$\frac{\hat{u}(y)}{X_g} = \mathrm{i}\,\omega_s^2 \int_0^y \frac{F(y')}{\mu(y')} dy' \,, \tag{13}$$

where $F(y)$ represents

$$F(y) = \int_H^y \frac{\rho(y')}{\delta_d(y')} dy' \,, \tag{14}$$

where y' represents a dummy integration variable. Nothing prevent this expression from being used to deal with layered stratum where there are stark contrasts between layers.

If one assumes, as it is customary, that the density is constant, then $\mu(y)/\rho = c_s^2(y) = (c_{s,base} f(\eta))^2$, and so is the damping δ_d too, eq. (13) boils down to

$$\frac{\hat{u}(\eta)}{X_g} = -\frac{\mathrm{i}}{\delta_d}\left(\frac{\omega_s}{c_{s,base}/H}\right)^2 \int_0^\eta \frac{(1-\eta')}{f^2(\eta')} d\eta' \,, \tag{15}$$

where, recall, $f(\eta) = c_s(y)/c_{s,base}$. It still remains to identify the value of the fundamental frequency, ω_s, to complete the previous expression. The estimate provided by the Rayleigh quotient, eq. (4), could be used. Hence, assuming once again the stiffness varies whereas the density and the damping stay constant across the stratum, we propose the following estimate for the fundamental frequency

$$\frac{\hat{u}(\eta)}{X_g} = -\mathrm{i}\,\frac{\mathcal{R}^2}{\delta_d} \int_0^\eta \frac{(1-\eta')}{f^2(\eta')} d\eta' \,, \tag{16}$$

This estimate is completely general, but it still requires a good guess of the mode shape (what may be difficult to ascertain in some cases, e.g., soft intermediate layers).

2.1.1. A dichotomy arising from the resonance argument

There is a consequential presupposition to be pointed out before going any further: eq. (11) represents equilibrium *point-wise*, that is, the forces therein are forces at a point on the cross-section, not the total force acting on the cross-section under consideration. The fact that *at one point* inertial and elastic forces balance does not entail necessarily that the same happens at all points in the cross-section simultaneously. In other words, it is not guaranteed that one was allowed integrate eq. (12) to obtain eq. (13) and subsequent, and therefore such result must be considered a simplification. There is a simple way of realizing this limitation: since elastic and inertial forces are equal, eq. (12) can be also written as

$$\mathrm{i}\delta_d\left(-\rho(y)\omega_s^2\hat{u}\right) = \rho(y)\ddot{X}_g = -\omega_s^2\rho(y)X_g \,, \tag{17}$$

hence an expression for the displacement, alternative to eq. (16), can be found from it:

$$\frac{\hat{u}}{X_g} = -\frac{\mathrm{i}}{\delta_d}\,, \tag{18}$$

which, evidently, may hold at the point level but it cannot be extended to the whole layer as it would not satisfy the boundary conditions at the base, hence eq. (16) and eq. (18) cannot hold simultaneously at all points of the vertical section.

Let us pause briefly to appreciate the meaning of eq. (18): it indicates that a point that is undergoing resonance experiences a relative displacement equal to the displacement at the base divided by the damping factor, and a change of phase of half a period. See that both eq. (18) and eq. (16) assign the same phase lag to to "resonating points".

2.2. Fundamental frequency and equivalent shear modulus

The dichotomy discussed in section 2.1.1 yields two contradictory displacement expressions, eq. (15) and eq. (18). One could think of reconciliating them, and such equality would yield an expression for the fundamental frequency. Such approach does not provide a functioning expression, but it inspires an alternative strategy nonetheless: consider the resonance amplitude, in terms of relative displacement in the homogeneous stratum, from eq. (6b), the fundamental resonant amplitude at the free-surface can be approximated as [18]

$$\frac{\hat{u}(\eta = 1)}{X_g} \approx \frac{4}{\pi\delta_d} - 1 \approx \frac{4}{\pi\delta_d}\,, \tag{19}$$

where it is assumed that $\delta_d \ll 1$, and then equate this expression to the modulus of eq. (15) to find ω_s and *the equivalent homogeneous shear modulus so that the inhomogeneous deposit resonates as a homogeneous layer*:

$$\frac{4}{\pi} \approx \left(\frac{\omega_s}{c_{s,base}/H}\right)^2 \int_0^1 \frac{(1-\eta)}{f^2(\eta)} d\eta \tag{20a}$$

$$\rightarrow \omega_s \approx \frac{c_{s,base}}{H} \Big/ \sqrt{\frac{\pi}{4} \int_0^1 \frac{(1-\eta)}{f^2(\eta)} d\eta} = \frac{\pi}{2}\frac{c_{s,eq}}{H}\,, \tag{20b}$$

whence

$$c_{s,eq} = \sqrt{\frac{\mu_{eq}}{\rho}} \rightarrow \mu_{eq} = \left(\frac{\pi^3}{16} \int_0^H \frac{(z/H)}{\mu(z)} d(z/H) \right)^{-1} . \tag{21}$$

Thus the inhomogeneous system undergoing resonance behaves as an homogeneous one presenting an equivalent shear modulus which corresponds to a linearly-weighted harmonic mean of the inhomogeneous distribution. See that these linear weights ($\pi^3 z/16 \approx 1.94z$) favor the contribution of the lower layers, $z/H \approx 1$, over the layers closer to the surface, $z/H \approx 0$, in other words, the integral consigns the dominance of the bottom properties over those close to the free surface insofar the fundamental response concerns.

This result differs fundamentally from the one that was obtained when considering the long-wavelength limit, eq. (9) , wherein the equivalent homogeneous property happened to be the harmonic mean of the shear-wave velocity, although both results would agree in the case they were applied to the homogeneous stratum directly.

2.3. Base-to-top amplification during resonance

Let us proceed to use eq. (16) top to obtain the amplification during resonance, ignoring the phase difference:

$$A_{est}(\omega_s) = \frac{X_g + |\hat{u}|}{X_g} = 1 + \frac{\mathcal{R}^2}{\delta_d} \int_0^1 \frac{(1-\eta)}{f^2(\eta)} d\eta \, . \tag{22}$$

Note how this results points out that the whole heterogeneity distribution affects the amplification. In order to check this estimate, consider homogeneous stratum, $f(\eta) = 1$, and the exact mode shape $\sin(\pi\eta/2)$:

$$A_{hom}(\omega_s) = 1 + \frac{1}{\delta_d} \frac{\pi^2}{8} \approx \frac{1.23}{\delta_d} \, , \tag{23}$$

where 1 has been neglected as it will be much smaller than the second, since $\delta_d \ll 1$ is presupposed. Comparing to the value suggested by Roesset [18], that is, $4/\pi\delta_d \approx 1.27/\delta_d$, it seems that, as it also happens in viscously-damped 1-dof systems [19], the maximum amplitude is slightly shifted towards a higher frequency due to the presence of damping. Nevertheless, the estimate, at least in this case, yields a value just about a 3% smaller.

Incidentally, the expression ω_s in eq. (20b) could be used to furnish another estimate, but this would yield simply the homogeneous value for amplification proposed by Röesset, eq. (19).

3. Comparison between exact and estimated response at resonance for profiles governed by "generalized parabola"

In the forthcoming sections, we shall focus our attention to verifying the estimates against results that assume a S-wave distribution given by eq. (3).

3.1. Displacement field

Figure 3 and Figure 4 display eq. (16) and eq. (18), as well as eq. (5) and eq. (6b), taking eq. (3) with $\beta = 0.1$ and $n = 0.1$ in the former and $\beta = 0.3$ and $n = 0.6$ in the latter. All expressions must be congruent, hence $+1$ has to be added to both eq. (16) and eq. (18) to obtain total displacements in all cases.

See that eq. (16) works fairly well when it comes to the magnitude in both cases. The phase is remarkable well approximated in both cases too.

One can acknowledge that, in spite of not satisfying the boundary condition at the base, eq. (18) captures a kind of average displacement across the layer, and that its phase coincide the actual one at the upper slices of the layer. This suggests that the upper points, those closer to the free-surface, are indeed undergoing "scalar resonance", as depicted in the rightmost force diagram in Figure 2 (and with the implications discussed earlier), during the actual resonance of the whole system.

A comparison to the displacement field of the homogeneous stratum, based on the properties at the base, has also been included, the reasons for this comparison shall become apparent in the later on, for now, the reader may appraise the striking resemblance, in both magnitude and phase, between eq. (5) and the homogeneous layer having $c_s(y) = c_{s,base}$ =constant, especially when $n = 0.1$,

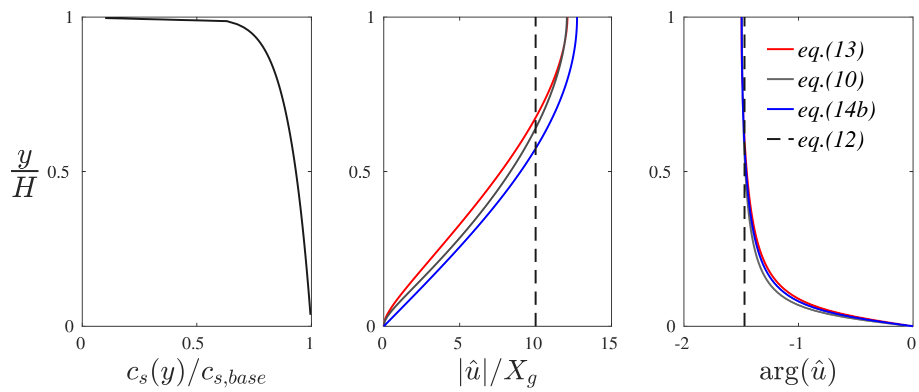

Figure 3: Comparison (exact, exact homogeneous and estimates) of displacement field across the stratum during resonance: left, S-wave velocity evolution ($n = 0.1$, $\beta = 0.1$); middle, magnitude of displacement during resonance; right, phase of displacement during resonance.

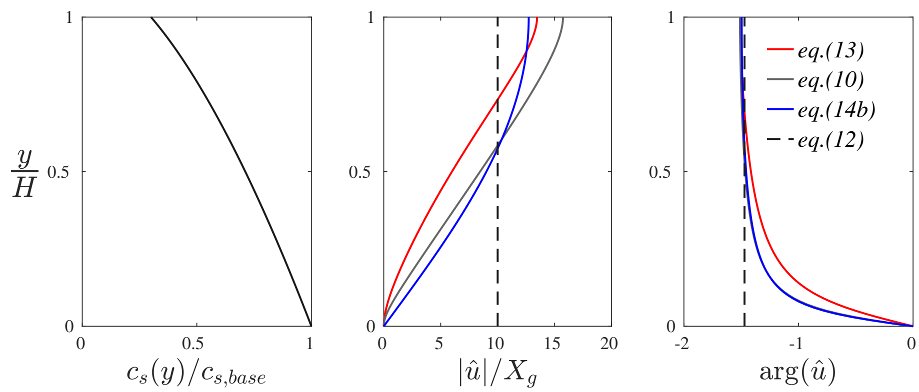

Figure 4: Comparison (exact, exact homogeneous and estimates) of relative displacement field across the stratum during resonance: left, S-wave velocity evolution ($n = 0.6$, $\beta = 0.3$); middle, magnitude of displacement during resonance; right, phase of displacement during resonance.

not so much when $n = 0.6$. The phase difference between the exact solution, eq. (5), and the homogeneous, eq. (6b), is almost negligible. This observation will be substantiated in Section 4.

3.2. Fundamental frequency

As a token of suitability, assume a profile given by eq. (3) and consider Figure 5: the exact solution of eq. (2) [12], the one based on applying Rayleigh quotient, eq. (4) (assuming a parabolic mode shape), the newly-obtained ex-

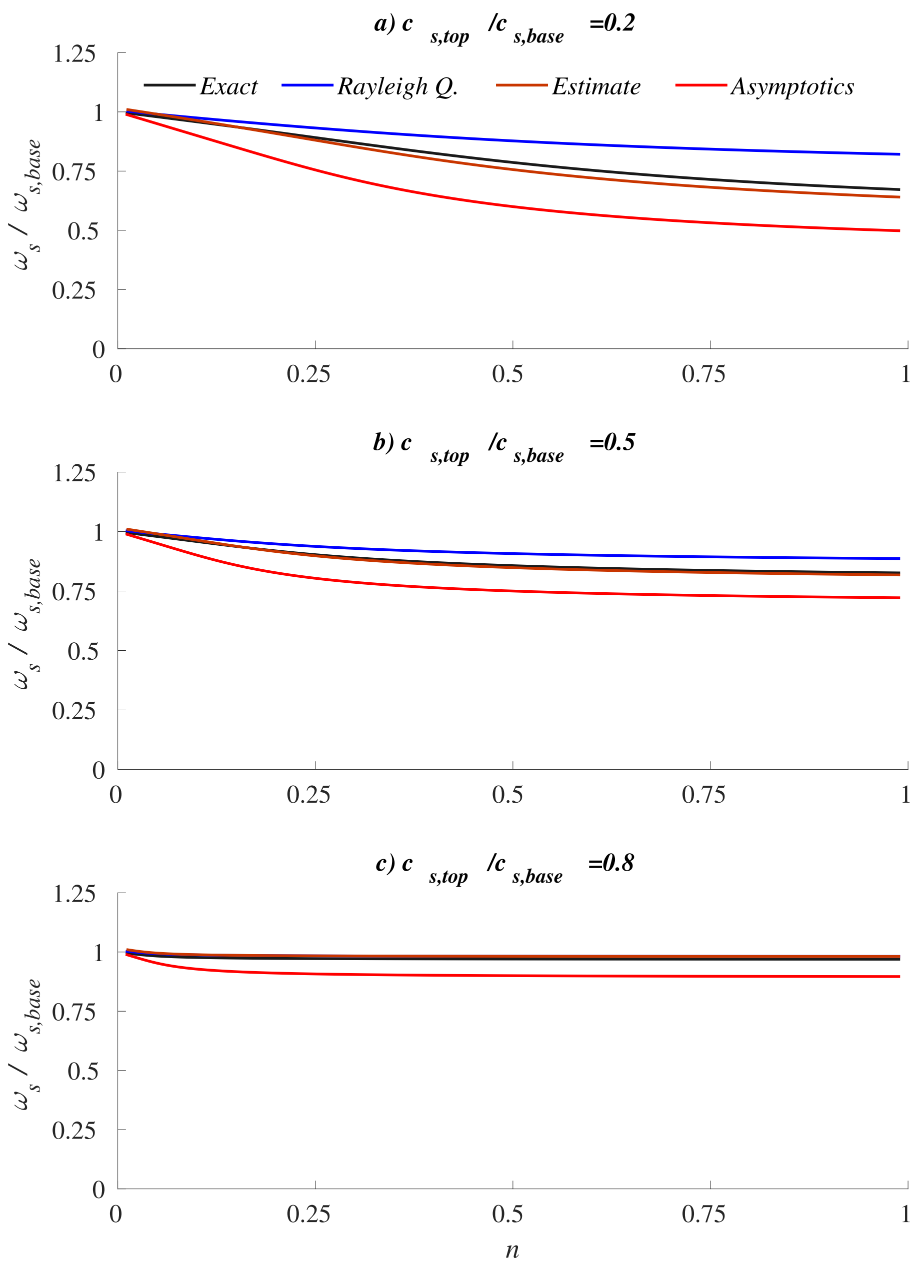

Figure 5: Comparison of fundamental frequency: estimate provided by the authors previously (*Asymptotics*) [16], eq. (4) (*Rayleigh Q.*), the newly-derived result eq. (20b) (*Estimate*), roots of denominator of eq. (5) (*Exact*).

pression eq. (20b) and the approximate eq. (10) ($k = 1$, which corresponds to what is termed *nominal frequency of the site* [7]) are compared in terms of the value that they yield for the fundamental frequency of the inhomogeneous layer ω_s, which is non-dimensionalized with the fundamental frequency of the homogeneous stratum based on properties at the base, $\omega_{s,base} = \pi c_{s,base}/2H$. The estimate based on Rayleigh quotient eq. (4) satisfactorily approximates the exact solution yet not as accurately as eq. (20b), whereas the estimate based in asymptotics (nominal frequency of the site), despite working well for higher modes, never performs as satisfactorily for the fundamental mode.

3.3. Base-to-top amplification

A comparison of the performance of both eq. (22) with eq. (4) and eq. (19) with eq. (20b) against eq. (7) and eq. (8) is desirable. Before being able to deliver it, the integral in eq. (22) must be evaluated using $f(\eta)$ as given in eq. (3):

$$\int_0^{\eta} \frac{(1-\eta')}{f^2(\eta')} d\eta' = \frac{1 - 2\alpha^{\frac{1}{2n}} + 2n\left(\alpha^{\frac{1}{2n}} - 1\right)}{2(n-1)(2n-1)\left(\alpha^{\frac{1}{2n}} - 1\right)^2} + $$
$$+ \frac{\left(\eta + \alpha^{\frac{1}{2n}}(-\eta + 2(\eta-1)n + 2) - 2(\eta-1)n - 1\right)\left(\eta\left(\alpha^{\frac{1}{2n}} - 1\right) + 1\right)^{1-2n}}{2(n-1)(2n-1)\left(\alpha^{\frac{1}{2n}} - 1\right)^2} . \tag{24}$$

The expression for the Rayleigh Quotient (assuming parabolic shape $\psi_1 = \eta^2/2 - \eta$) is available in the literature [14]. Figure 6 displays the comparison.

The estimates for the fundamental mode amplitude work fairly well in all three cases, as reported in the following table:

Parameters	*Equation* (7)	*Equation* (19)	*Equation* (22)
$n = 0.5$, $\beta = 0.9$, $\delta_d = 0.15$	8.6	8.5 (-1.3%)	8.6 ($<$0.1%)
$n = 0.5$, $\beta = 0.5$, $\delta_d = 0.10$	13.7	12.7 (-7.3%)	14.6 (+6.6%)
$n = 0.5$, $\beta = 0.1$, $\delta_d = 0.05$	31.0	25.5 (-17.8%)	36.2 (+16.8%)

Table 1: Amplitudes at the fundamental mode for three models ($n = 0.5$) and different contrast and damping (the number in parenthesis represent percent deviation from eq. (7), the exact solution).

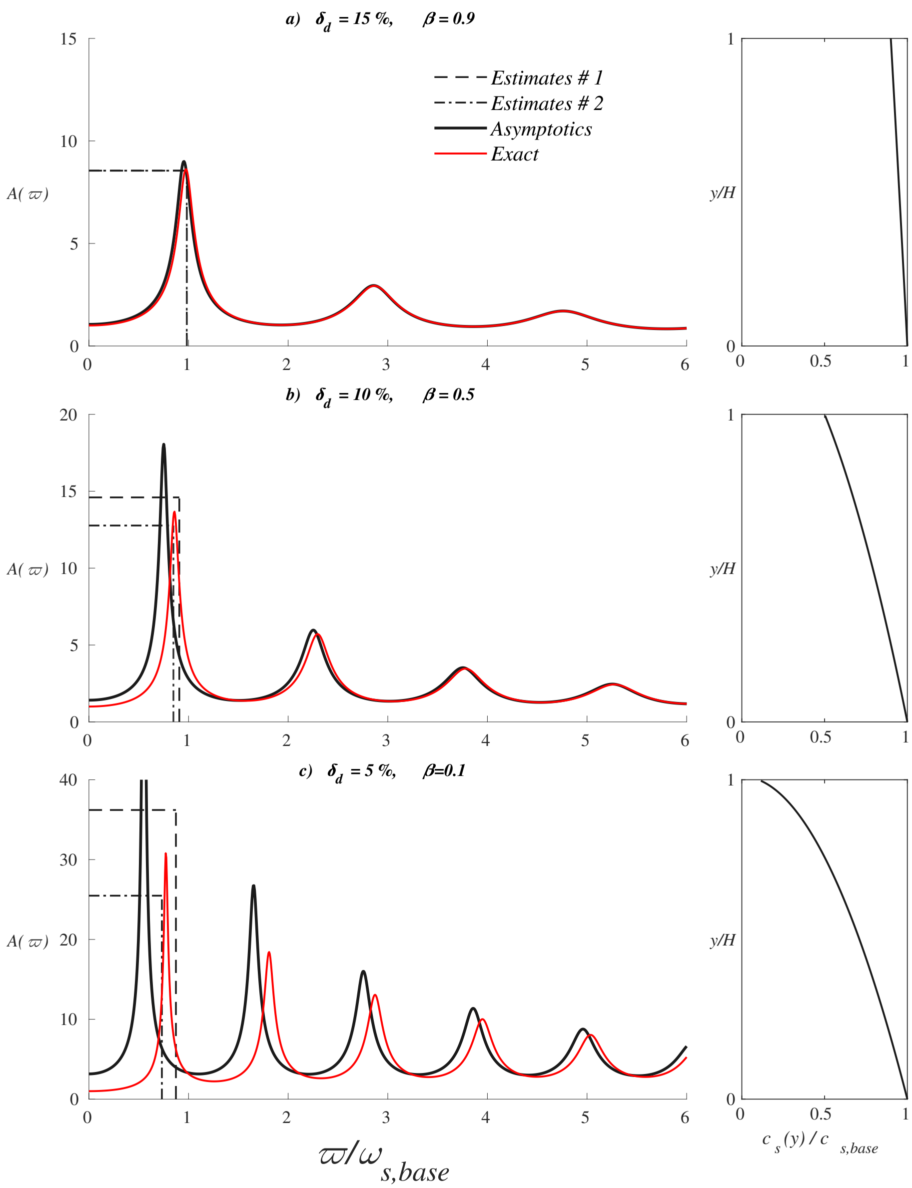

Figure 6: Base-to-top dynamic amplification $A(\varpi)$ (with corresponding vertical S-wave profile $c_s(y)$), comparison between eq. (22) with eq. (4) (*Estimates #1*), eq. (19) with eq. (20b) (*Estimates #2*), eq. (7) (*Exact*), and eq. (8) (*Asymptotics*) for inhomogeneity factor $n = 0.5$ and different damping values.

The error increases as the inhomogeneity increases (maximum error around 17%, overestimation and underestimation depending on the estimate). See how this amplitude misfit goes associated to an overestimation of the fundamental frequency, hence improving the estimate for the latter (e.g. using a sinusoidal mode shape instead of a parabolic one) would return also a better estimate of the former. The data regarding the fundamental frequency estimation is already consigned in Figure 5.

One should highlight that using eqs. (19) and (22) in conjunction with eq. (4) for the fundamental mode while using eq. (8) for the higher modes may provide decent estimates of the whole range of frequency behavior for these systems in some cases.

4. Particularization for profiles with acute gradients of stiffness localized in upper layers

In many practical cases, there is evidence of substantial stiffness changes being confined in a narrow region close to the surface; once this first zone of rapid growth of stiffness is left behind, the stiffness continues increasing with depth yet at slower pace. This behavior adjusts better to values of the inhomogeneity factor $n \leq 0.1$.
Let us re-assess eq. (22) bringing this fact to bear.

a) In first place, as $\mathcal{R}$ depends on the integral of the mode shapes, if most inhomogeneity is intensely localized in a narrow upper layer, whereas in the rest of the domain is similar to the one at the base, it seems logical to assume that the shape will resemble the one of the homogeneous profile except at a narrow region at the top. However, as the quotient entails a *global* comparison to the exact shape (through the integral), as opposed to point-wise local comparison, then we argue the value of the integrals will not differ too much from the one of the homogeneous stratum with properties as at the base, and hence $\mathcal{R} \approx \pi/2$.

b) A similar, even-more-convincing argument can be leveled at the integral factor in eq. (22): see how the integral was argued to represent an averaged compliance wherein the weights start from zero at the surface and increase the deeper the point under consideration; this means the integral weights automatically diminish the contribution of the upper narrow region where the stiffness differ the most from the one at the base. Hence, under these circumstances, this integral value must be controlled by the value at the base (which has the most favorable weighting and it is, by the assumption $n \leq 0.1$, the largest), then the integral value must be close to the value corresponding to $f(\eta) = 1$ (the whole stratum having base stiffness).

Let us deploy this arguments within eq. (22):

$$A_{est}(\omega_s) \approx 1 + \frac{\pi^2}{4\delta_d} \int_0^1 \frac{(1-\eta)}{1} d\eta = 1 + \frac{\pi^2}{8\delta_d} \, . \tag{25}$$

This is the same result that we obtained in eq. (23), that is, when we used the formula to calculate the amplification corresponding to the homogeneous layer. See that this expression does not require a prior estimate of the natural frequency, unlike eq. (22).

The conclusion is that, for the case when n is relatively small, the behavior of the inhomogeneous stratum shall resemble the one of the homogeneous one having as mechanical properties those of the bottom (base) layer. Under these premises, the response of the fundamental mode can be considered as independent of both the contrast, i.e., β, and the fine details of the distribution of shear-wave velocity, i.e., exact value of n (provided that $n < 0.1$ to begin with). In order to better appraise this corollary, revisit the results in Figure 3 and Figure 4 in light of this premise, particularly the middle tile in Figure 3.

4.1. Verification for profiles governed by "generalized parabola"

For instance, compare the value that the estimate would deliver ($\delta_d = 0.05$) for the fundamental mode to those of eq. (7), which are shown in next table for different combinations of β and n.

	Top-to-base contrast (β)		
Inhomogeneity factor (n)	0.1	0.5	0.9
0.9	33.8	27.2	25.6
0.5	30.8	27.1	25.5
0.1	26.0	26.0	25.5

Table 2: Exact amplitude at the fundamental mode for a number of models, from eq. (7).

Whereas the estimate from eq. (25) is

$$A_{est}(\omega_s) \approx 1 + \frac{\pi^2}{8 \cdot 0.05} \approx 1 + \frac{1.23}{0.05} = 25.6\,. \tag{26}$$

All the prior results concern $\delta_d = 0.05$.The maximum error, is 24.3% (amplitude is underestimated), but it corresponds to $n = 0.9$ and $\beta = 0.1$, a 90% decrease in stiffness happening almost linearly, then the premises upon which the reasoning was developed (gradient localized at the top) does not hold in any way, shape or form.

Is interesting to note that for $\beta = 0.5$ still get less than 10% error (underestimation), we ascribe this to the helpful effect on the weight in the integral factor. Likewise, as long as $n = 0.1$, the error is just testimonial. Again, the agreement is credited to the weights of the integral favoring the bottom layers.

Clearly, the trends that were predicted from eq. (25) are the ones observed.

4.2. Verification for discontinuous velocity profile

Hitherto, everything has been referred to profiles under the umbrella of the "generalized parabola", eq. (3), but, as it has already been pointed out, one could work directly with the down-hole data since there are no requirements of any kind over continuity in mechanical properties profile to evaluate the integral the expressions of the estimates depend on. The estimate (25) should work well if the same conditions discussed above are met: heterogeneity concentrated in upper layer.

In order to illustrate this point, let us pick three real profile from the Kiban-Kyoshin Network (*KiK-net*) database [20]. One being used corresponds to

Kasumigaura station (Ibaraki prefecture), code name IBRH17, another one from Taiki (Tokachi Subprefecture, Hokkaido) and the last one from Ishige (Yuki District, Ibaraki Prefecture). The available borehole data is displayed (as provided) in the next tables:

No.	Thickness (m)	Depth (m)	c_p (m/s)	c_s (m/s)
1	1.00	1.00	160	90
2	9.00	10.00	500	250
3	80.00	90.00	1700	380
4	145.00	235.00	1700	470
5	65.00	300.00	1900	540
6	80.00	380.00	1900	660
7	80.00	460.00	2100	820
8	–	–	5300	2300

Table 3: Information concerning KiK-net site IBRH17

No.	Thickness (m)	Depth (m)	c_p (m/s)	c_s (m/s)
1	4.00	4.00	300	130
2	32.00	36.00	1850	480
3	42.00	78.00	1850	590
4	22.00	100.00	5000	2800

Table 4: Information concerning KiK-net site TKCH08

No.	Thickness (m)	Depth (m)	c_p (m/s)	c_s (m/s)
1	20.00	20.00	540	110
2	170.00	190.00	1560	380
3	220.00	410.00	1800	530
4	108.00	518.00	2150	850
5	182.00	700.00	4360	2350
6	–	–	0	0

Table 5: Information concerning KiK-net site IBRH10

Let us point out that these three sites are classified as “LG” according to the taxonomy proposed by Thompson and collaborators [21], what entails that these results, derived from the one-dimensional linear-elastic assumption, can inform realistic estimates for amplification in these sites (more realistic data regarding damping at specific sites). In addition, consider the last layer in each case as rigid bedrock, then calculate the transfer function numerically following the classic methodology (give, for instance, in[15]). The calculation result is contained in Figure 7, the damping values used have been $\delta_d = 0.147$ for IBRH17, 0.068 for TKCH08 and 0.035 for IBRH10.

As it can be seen from inspecting Figure 7, the value of the natural frequency is remarkably well estimated by eq. (20b), not only the second case (TKCH08) which is the one that would better adjust to $n \ll 1$, but also the other two. The performance of eq. (20b) estimating the fundamental frequency of the sites and is assessed qualitatively in the following table:

	$\omega_s/\omega_{s,base}$		$A(\varpi = \omega_s)$	
Sites	Numerical	Estimate	Numerical	Estimate
IBRH17	0.73	0.73 (-1.3%)	9.33	9.39 (+0.6%)
TKCH08	0.96	0.94 (-2.1%)	20.5	19.1 (-6.8%)
IBRH10	0.68	0.67 (-1.5%)	37.9	36.3 (-4.2%)

Table 6: Amplitudes at the fundamental mode for three KiK-net model in Figure 7 (the number in parenthesis represent percent deviation from numerical result).

Thus the amplitude error ranges from less than 1% (overestimation) to less than 8% at most (underestimation). In similar fashion, the error in (under)estimating the fundamental frequency is arounf 2% of the numerically-obtained value.

5. Conclusions and future work

Conclusions

This work main objective has been to deliver simple estimates for the response of an inhomogeneous soil layer overlying rigid bedrock, subjected to incoming SH

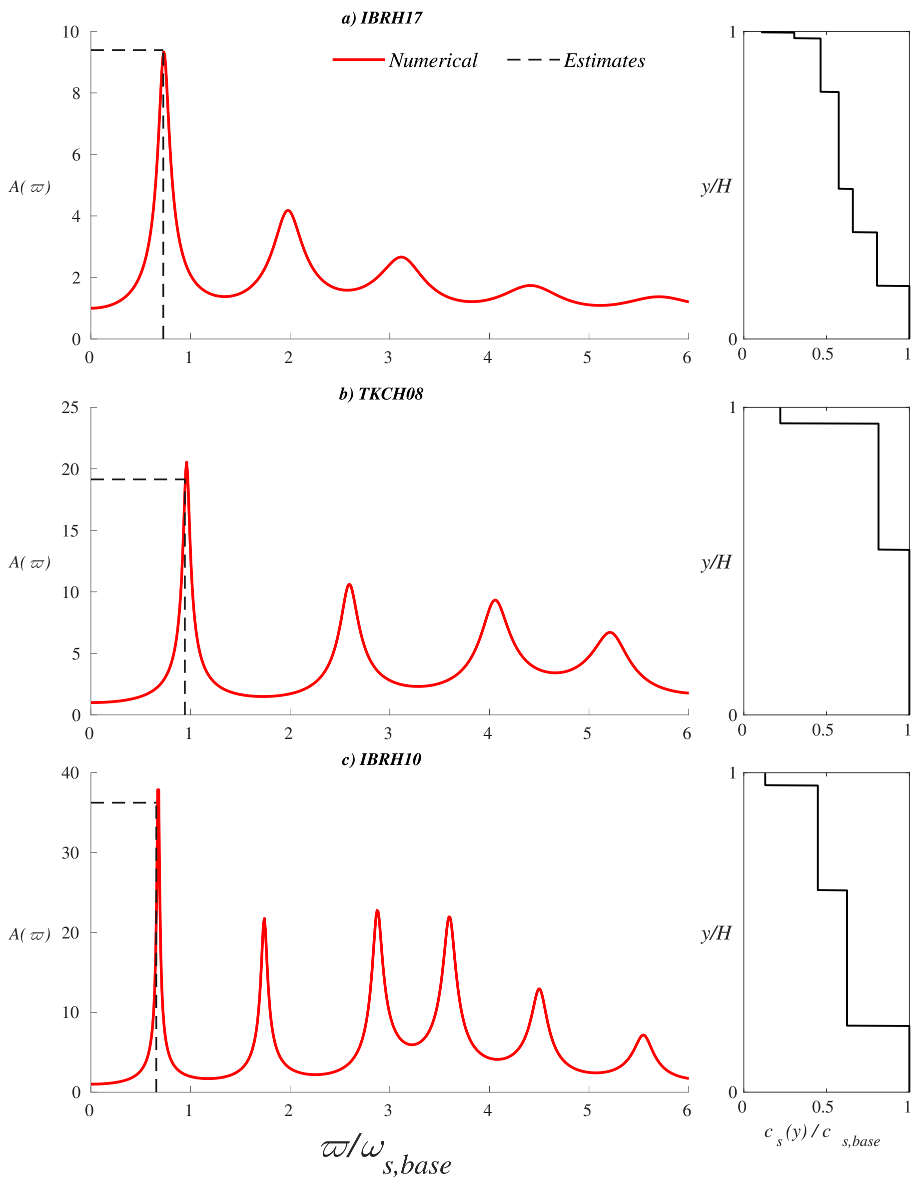

Figure 7: Transfer function and profile corresponding to KiK-net sites (discontinuous line marks the estimate eq. (25)).

waves which excite the fundamental resonance mode of the stratum. Customary simplifying assumptions (linear-elastic response, vertically-layered medium, SH wave-front, frequency-independent damping) are taken to be in effect.

The expression eq. (22) is valid for soils having any stiffness (although it requires a good frequency estimate $\mathcal{R}$), whereas eq. (25) is adequate to estimate such amplitude for any distribution wherein the main stiffness gradients happen relatively close the surface.
Regarding estimation of the fundamental frequency of the site, eq. (20b) has proved to work satisfactorily in both scenarios concerning continuous profiles and sites presenting discontinuous profiles with sudden jumps.

Future work

The first path to improvement must be adding radiational damping [15], what would extend the applicability of the results from a limited number of strata having large impedance contrast (effective rigid bedrock) to any two horizontal sections in a layered half-space.

A two-layer system resting on bedrock [12], another classic configuration, may also be readily used to expand these results (intuition hints that the estimate eq. (25) will perform satisfactorily in these cases, based on the argumentation carried out in section 4).

Insofar mechanical properties distribution is concerned, one should re-stress that the expression eq. (22) is completely general, so actually any velocity profile could be used, including those that present stiffness reversal (soft intermediate layers), but it requires an estimate of the fundamental frequency (e.g. the Rayleigh quotient), what may not be always easy to obtain. On the other hand, it also remains to be verified that eq. (20b) works in scenarios presenting either increasing stiffness gradients ($\beta > 1$) or intermediate softer layers.

Once again, the previous results were derived under very specific suppositions, see section 1. One of those presuppositions is linear-elastic behavior. The possibility of extending the argument used in section 2 to the non-linear regime is enticing and should be explored.

References

[1] L. Benuska, Ground motion, loma prieta earthquake reconnaissance report, Earthquake Spectra 6 (1990) 25–80.

[2] I. Towhata, Seismic wave propagation in elastic soil with continuous variation of shear modulus in the vertical direction, Soils and Foundations 36 (1) (1996) 61–72.

[3] R. Dobry, R. V. Whitman, J. M. R. Vinuesa, Soil properties and the one-dimensional theory of earthquake amplification, MIT Department of Civil Engineering, Inter-American Program, 1971.

[4] G. Gazetas, Vibrational characteristics of soil deposits with variable wave velocity, International journal for numerical and analytical methods in Geomechanics 6 (1) (1982) 1–20.

[5] C. Vrettos, Dynamic response of soil deposits to vertical sh waves for different rigidity depth-gradients, Soil Dynamics and Earthquake Engineering 47 (2013) 41–50.

[6] C. Vrettos, Dispersive sh-surface waves in soil deposits of variable shear modulus, Soil Dynamics and Earthquake Engineering 9 (5) (1990) 255–264.

[7] J. Zhao, Modal analysis of soft-soil sites including radiation damping, Earthquake engineering & structural dynamics 26 (1) (1997) 93–113.

[8] H. Afra, A. Pecker, Calculation of free field response spectrum of a non-homogeneous soil deposit from bed rock response spectrum, Soil Dynamics and Earthquake Engineering 22 (2) (2002) 157–165.

[9] T. Travasarou, G. Gazetas, On the linear seismic response of soils with modulus varying as a power of depth: the maliakos marine clay, Soils and foundations 44 (5) (2004) 85–93.

[10] J. Semblat, A. Pecker, Waves and vibrations in soils, Earthquakes, traffic, shocks.

[11] S. Sarma, Analytical solution to the seismic response of visco-elastic soil layers, Geotechnique 44 (2) (1994) 265–275.

[12] E. Rovithis, H. Parashakis, G. Mylonakis, 1d harmonic response of layered inhomogeneous soil: Analytical investigation, Soil Dynamics and Earthquake Engineering 31 (7) (2011) 879–890.

[13] P. Dakoulas, G. Gazetas, A class of inhomogeneous shear models for seismic response of dams and embankments, International Journal of Soil Dynamics and Earthquake Engineering 4 (4) (1985) 166–182.

[14] G. E. Mylonakis, E. Rovithis, H. Parashakis, 1d harmonic response of layered inhomogeneous soil: exact and approximate analytical solutions, in: Computational Methods in Earthquake Engineering, Springer, 2013, pp. 1–32.

[15] S. L. Kramer, Geotechnical earthquake engineering. in Prentice–Hall international series in civil engineering and engineering mechanics, Prentice Hall Inc., Englewood Cliffs, New Jersey, 1996.

[16] J. Garcia-Suarez, E. Esmaeilzadeh, D. Asimaki, Seismic harmonic response of inhomogeneous soil: scaling analysis, Géotechnique.

[17] G. W. Housner, D. E. Hudson, Applied mechanics: dynamics, Vol. 1, Van Nostrand, 1959.

[18] J. Roesset, Soil amplification of earthquakes, Numerical methods in geotechnical engineering (1977) 639–682.

[19] R. Clough, J. Penzien, Dynamics of Structures, 2nd York, 1992.

[20] Y. Okada, K. Kasahara, S. Hori, K. Obara, S. Sekiguchi, H. Fujiwara, A. Yamamoto, Recent progress of seismic observation networks in japan—hi-net, f-net, k-net and kik-net—, Earth, Planets and Space 56 (8) (2004) xv–xxviii.

[21] E. M. Thompson, L. G. Baise, Y. Tanaka, R. E. Kayen, A taxonomy of site response complexity, Soil Dynamics and Earthquake Engineering 41 (2012) 32–43.